

Improved low-temperature rate constants for rotational excitation of CO by H₂

M. Wernli¹, P. Valiron¹, A. Faure¹, L. Wiesenfeld¹, P. Jankowski², and K. Szalewicz³

¹ Laboratoire d'Astrophysique de Grenoble, UMR 5571 CNRS-UJF, OSUG, Université Joseph Fourier, BP 53, F-38041 Grenoble Cedex 9, France

² Department of Quantum Chemistry, Institute of Chemistry, Nicolaus Copernicus University, Gagarina 7, PL-87-100 Toruń, Poland

³ Department of Physics and Astronomy, University of Delaware, Newark, DE 19716, USA

Received 26 July 2005 / Accepted 12 September 2005

Abstract. Cross sections for the rotational (de)excitation of CO by ground state para- and ortho-H₂ are obtained using quantum scattering calculations for collision energies between 1 and 520 cm⁻¹. A new CO–H₂ potential energy surface is employed and its quality is assessed by comparison with explicitly correlated CCSD(T)-R12 calculations. Rate constants for rotational levels of CO up to 5 and temperatures in the range 5–70 K are deduced. The new potential is found to have a strong influence on the resonance structure of the cross sections at very low collision energies. As a result, the present rates at 10 K differ by up to 50% with those obtained by Flower (2001) on a previous, less accurate, potential energy surface.

Key words. molecular data – molecular processes – ISM: molecules

1. Introduction

Since its discovery in interstellar space more than 30 years ago (Wilson et al. 1970), carbon monoxide (CO) has been extensively observed both in our own and in other galaxies. CO is indeed the second most abundant molecule in the Universe after H₂ and, thanks to its dipole moment, it is the principal molecule used to map the molecular gas in galactic and extragalactic sources. CO is also currently the only molecule to have been observed at redshifts as high as $z = 6.42$ (Walter et al. 2003). Collisional excitation of rotational levels of CO occurs in a great variety of physical conditions and emission from levels with rotational quantum numbers J up to 39 have been identified in circumstellar environments (Cernicharo et al. 1996).

Hydrogen molecules are generally the most abundant colliding partners in the interstellar medium, although collisions with H, He and electrons can also play important roles, for example in diffuse interstellar clouds. Rate coefficients for collisions with H₂ based on the potential energy surface (PES) of Jankowski & Szalewicz (1998, hereafter JS98) have been calculated recently (Mengel et al. 2001; Flower 2001). These rates were found to be in reasonable agreement (typically within a factor of 2 at 10 K) with those computed on older and less accurate PES (e.g. Schinke et al. (1985)). However, in contrast to previous works, Mengel et al. (2001) and Flower (2001) found the inelastic rates with $\Delta J = 1$ larger than those with $\Delta J = 2$

for para-H₂. This result reflects the crucial importance of the PES, whose inaccuracies are one of the main sources of error in collisional rate calculations, especially at low temperatures (see, e.g., Balakrishnan et al. (2002)). The JS98 surface has been checked against experiment by a couple of authors. Gottfried & McBane (2001), in particular, computed second virial coefficients below 300 K and showed that the attractive well of the PES was slightly too deep. A modification which consists of multiplying the PES by a factor of 0.93 was therefore suggested by these authors. This modification was applied by Mengel et al. (2001) and it was indeed found to produce better agreement with measurements of pressure broadening cross sections. On the other hand, the original PES was found to give a very good agreement with experimental state-to-state rotational cross sections measured near 1000 cm⁻¹ (Antonova et al. 2000). At these energies, however, only the short-range repulsive region of the PES is probed. Finally, Flower (2001) showed that the scaling of 0.93 has only minor influence on the rotational rates and he employed the original PES.

Very recently, a new PES has been computed by Jankowski & Szalewicz (2005) (hereafter JS05). In contrast to the JS98 surface, which was calculated within the symmetry-adapted perturbation theory (SAPT), the JS05 surface has been obtained using the supermolecular approximation based on the CCSD(T) method using correlation-consistent basis sets complemented by bonding functions and basis set extrapolation. It turned that the major inaccuracy of JS98 was due to the use of a correction for the effects of the third and higher orders ex-

tracted in an approximate way from supermolecular SCF calculations. It recently became clear that this correction should not be used for nonpolar or nearly nonpolar monomers. If this term is removed from JS98, the agreement of the resulting surface with JS05 is excellent. Jankowski & Szalewicz (2005) have employed their new PES to calculate rovibrational energy levels of the para-H₂-CO complex and they obtained a very good agreement (better than 0.1 cm⁻¹ compared to 1 cm⁻¹ for the JS98 surface) with the measurements by McKellar (1998). The computed values of the second virial coefficients also agree very well with the experimental ones. Full details can be found in Jankowski & Szalewicz (2005). In the present paper, we present new rate constants for the rotational excitation of CO by H₂ based on the JS05 surface. Our results are restricted to low temperatures ($T < 70$ K) because the new PES calculations are found to affect the rotational cross sections only at low collision energy ($E_{\text{coll}} < 60$ cm⁻¹). As shown below, differences with the results of Flower (2001) range from a few percent to 50 %. Such effects, if not dramatic, are significant in view of the special importance of the CO-H₂ system in astrophysics. Furthermore, the present results are of particular interest for comparisons with future measurements planned in Rennes by Sims and collaborators (Sims 2005).

2. Method

2.1. Potential Energy Surface

Following the conventions of JS98, the CO-H₂ “rigid-body” PES is described by the following four Jacobi coordinates: three angles θ_1 , θ_2 and ϕ and the distance R denoting the intermolecular centre of mass separation. The angles θ_1 and θ_2 are the tilt angles of H₂ and CO with respect to the intermolecular axis, and ϕ is the dihedral angle. In the linear geometry, the oxygen atom points toward H₂ when $\theta_2=0$. The JS05 surface has been obtained by averaging over the intramolecular ground state vibration of H₂, while CO was treated as rigid at its vibrational ground-state averaged geometry. The JS05 surface has a global depth of -93.049 cm⁻¹ for the linear geometry with the C atom pointing toward the H₂ molecule ($\theta_1 = 0$, $\theta_2=180^\circ$, $\phi = 0$) and for a centre of mass separation $R_{\text{min}} = 7.92$ bohrs. The (unscaled) JS98 and JS05 surfaces are presented in Fig. 1 and compared to independent CCSD(T)-R12 calculations using ground-state averaged geometries for CO and H₂.

The latter calculations can be considered as high accuracy state-of-the-art *ab initio* calculations. Indeed the CCSD(T)-R12 approach¹ has been shown to produce intermolecular energies with near spectroscopic accuracy without recourse to extrapolation (Halkier et al. 1999; Müller & Kutzelnigg 2000; Faure et al. 2005). In order to save some computing time and to improve the numerical stability of the R12 operator, the core or-

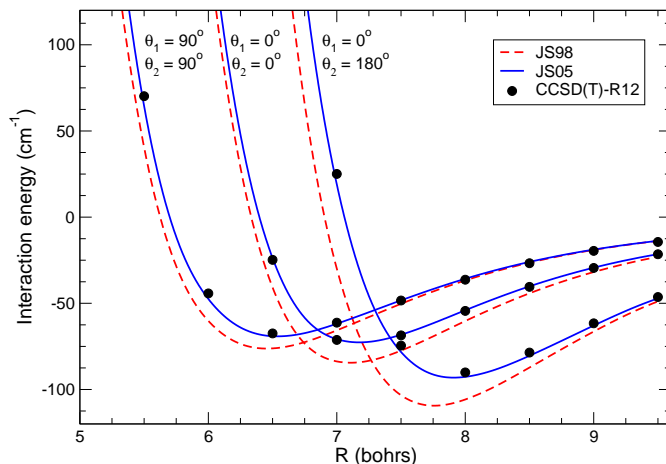


Fig. 1. H₂-CO interaction energy as a function of R for three coplanar configurations: $(\theta_1, \theta_2) = (90^\circ, 90^\circ)$, $(0^\circ, 0^\circ)$ and $(0^\circ, 180^\circ)$. The dashed and solid lines denote the JS98 and JS05 calculations, respectively. The filled circles correspond to independent CCSD(T)-R12 calculations (see text).

bitals were frozen² in the CCSD(T)-R12 calculations. We employed R12-suited basis sets including up to g functions for C and O, and d functions for H (as developed in Noga & Valiron (2003); Kedžuch et al. (2005)). The R12 results are assumed to approach the basis set limit within 1 – 2 cm⁻¹. In particular the inclusion of a large set of bonding functions (corresponding to the R12-suited H set) affects the interaction by ≈ 0.5 cm⁻¹ only at 7 bohrs separation, while the counterpoise corrections remain very small, generally below 1 cm⁻¹.

Here, we can observe that the JS05 surface agree very well with the CCSD(T)-R12 results while the JS98 surface overestimates the depth of the CO-H₂ potential well by about 10–20 %, as anticipated by Gottfried & McBane (2001). However, the JS05 surface lies slightly below the CCSD(T)-R12 one. This agrees with the observation in JS05, based on extrapolations involving bases up to quintuple zeta quality, that the potential is about 1-2 cm⁻¹ too deep in the region of the global minimum. On the other hand, the comparison of the virial coefficients from JS05 with experiment suggests that the exact potential is still deeper, probably due to the effects resulting from theory levels beyond CCSD(T). We also checked that the R12 values are recovered within 1 cm⁻¹ by a basis set extrapolation involving larger (triple and quadruple zeta) sets and the popular bonding functions proposed by Williams et al. (1995). These comparisons provides a further check of the quality of the new CO-H₂ PES and also confirm the suspected inaccuracies of the JS98 surface.

In order to interface the JS98 and JS05 surfaces with the scattering code, the FORTRAN routines of Jankowski & Szalewicz (1998); Jankowski & Szalewicz (2005) were employed to generate a grid of 57,000 geometries. These grid points were distributed in 19 fixed intermolecular distances R (in the range 4–15 bohrs) via random sampling

¹ The R12 coupled cluster theory with singles, doubles and perturbative triples properly describes the electron-electron cusp by including explicitly the inter-electronic coordinates into the wavefunction (Noga & Kutzelnigg (1994), see also Noga & Valiron (2002) for a review.)

² This approximation is of little consequence as core correlation effects are minor for the CO-H₂ interaction (about 0.3 cm⁻¹ at 7 bohrs separation).

for the angular coordinates. At each intermolecular distance, the interaction potential V was least-squares fitted over the following angular expansion:

$$V(R, \theta_1, \theta_2, \phi) = \sum_{l_1 l_2 l} v_{l_1 l_2 l}(R) s_{l_1 l_2 l}(\theta_1, \theta_2, \phi), \quad (1)$$

where the basis functions $s_{l_1 l_2 l}$ are products of spherical harmonics and are explicated in Eq. (A9) of Green (1975). These functions form an orthonormal basis set, and the expansion coefficients $v_{l_1 l_2 l}$ can thus be written as³

$$v_{l_1 l_2 l}(R) = \int_{\theta_1} \int_{\theta_2} \int_{\phi} V(R, \theta_1, \theta_2, \phi) s_{l_1 l_2 l}^*(\theta_1, \theta_2, \phi) \sin \theta_1 d\theta_1 \sin \theta_2 d\theta_2$$

The latter expression remains valid for any truncated expansion.

We selected an initial angular expansion including all anisotropies up to $l_1=10$ for CO and $l_2=6$ for H₂, resulting in 142 $s_{l_1 l_2 l}$ functions. The accuracy of the angular expansion was monitored using a self-consistent Monte Carlo error estimator (Rist et al. 2005), which also permitted to select the most pertinent angular terms. The resulting set was composed of 60 basis functions involving anisotropies up to $l_1 = 7$ and $l_2 = 4$. A cubic spline interpolation was finally employed over the whole intermolecular distance range and was smoothly connected with standard extrapolations to provide continuous expansion coefficients suitable for scattering calculations. The final accuracy of this 60 term expansion was found to be better than 1 cm⁻¹ in the global minimum region of the PES while the individual expansion coefficients were converged within 0.01 cm⁻¹. It should be noted that the expansion does not reproduce exactly the values of the potential energy at the grid points⁴, in contrast to the approach followed by Flower (2001) who used the same number (25) of angular geometries and basis functions. The main advantage of our approach is to guarantee the convergence of the individual expansion coefficients, in particular in the highly anisotropic short-range part ($R < 6$ bohrs) of the interaction.

2.2. Scattering calculations

The MOLSCAT code (Hutson & Green 1994) was employed to perform the rigid-rotor scattering calculations reported below. All calculations were made using the rigid rotor approximation, with rotational constants $B_{\text{CO}} = 1.9225$ cm⁻¹ and $B_{\text{H}_2} = 60.853$ cm⁻¹. For para-H₂ ($j_2 = 0$), calculations were carried out at total energies (collision plus CO rotation) ranging from 4 to 520 cm⁻¹. Full close-coupling calculations were performed between 4 and 160 cm⁻¹, with steps of 0.2 cm⁻¹ in the resonance range 4–120 cm⁻¹, and a much coarser step of 5 cm⁻¹ between 120 and 160 cm⁻¹. Between 160 and 520 cm⁻¹, the coupled-state approximation (McGuire & Kouri 1974) was shown to reproduce full close-coupling calculations within a few percent

³ ★ denotes the complex conjugate. Note that the angular conventions of Green (1975) are slightly different from those of Jankowski & Szalewicz (1998).

⁴ The residual differences indicate the cumulative effects of the higher expansion terms.

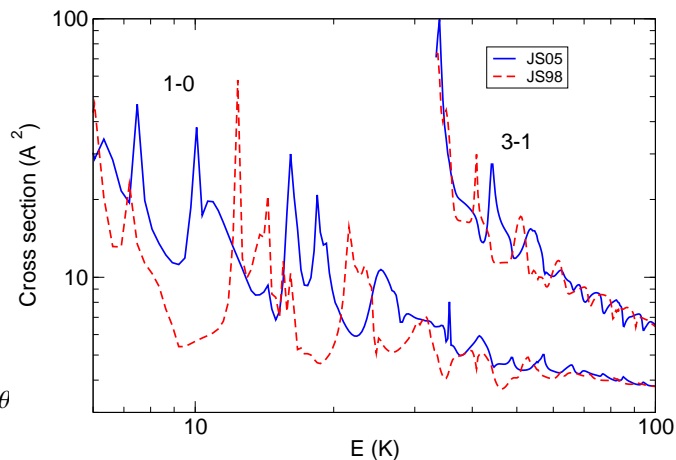


Fig. 2. Inelastic deexcitation cross sections for CO in collisions with para-H₂ as a function of total energy. Both curves are the results of our calculations with the unscaled JS98 PES (dashed curves), and the JS05 PES (solid curves).

and was thus employed. The energy step was 20 cm⁻¹ between 160 and 340 cm⁻¹, and 30 cm⁻¹ at higher energies. For ortho-H₂, the same collision energy grid was used, resulting in total energies in the range 126–642 cm⁻¹. The propagator used was the log-derivative propagator (Alexander & Manolopoulos 1987). Parameters of the integrator were tested and adjusted to ensure a typical precision of 1-2 %. All the calculations with para-H₂ used a $j_2 = 0, 2$ basis, while the ortho-H₂ calculations used only a $j_2 = 1$ basis. Tests of this basis were made at the highest energy, where inclusion of the $j_2 = 3$ (closed) state was found to affect cross sections by less than one percent. At least three closed channels were included at each energy for the CO rotational basis. At the highest energy, we had thus a $j_1 \leq 18$ basis. Transitions among all levels up to $j_1 = 5$ were computed. Finally, rate constants were calculated for temperatures ranging from 5 to 70 K by integrating the cross sections over essentially the whole collision energy range spanned by the corresponding Maxwell-Boltzmann distributions. The energy grid was chosen so that the highest collision for all transitions be about ten times larger than the highest temperature. The accuracy of the present rates is expected to lie between 5 and 10 % at 70K, and probably better at lower temperatures.

3. Collisional cross sections and rates

Figure 2 clearly illustrates the fact that the resonance pattern, which is here of 'shape' rather than 'Feshbach' type as discussed by Flower (2001), strongly depends on the interaction potential. We also note that the very fine grid used at the lowest energies was necessary for a proper description of the resonances. It can be observed that the cross sections converge at higher energies (above the resonance regime), as the collision energy becomes large compared to the potential energy well depth. As a result, rate constants are expected to differ significantly from those of Flower (2001) at very low temperatures only.

We present in Tables 1 and 2 our rate constants at 10, 30 and 70 K, and those of Flower (2001) for comparison. We note

that especially at 10 K, rates can vary up to 50%. These differences reflect the influence of three independent parameters: (i) the high accuracy of the new *ab initio* potential energy calculations, (ii) the use of a well converged expansion of the PES over the angular basis functions and (iii) the careful description of resonances. It is however not clear how to discriminate among the three effects. At 70K (and beyond), our rates and those of Flower (2001) agree within typically 10–20 %, as anticipated from the convergence of the cross sections at high energy. We therefore conclude that the differences between our results and those of Flower (2001) are astrophysically relevant for temperatures below 70 K. Above this value, the inaccuracies of the JS98 PES have only a minor influence on the rotational rates and the results of Flower (2001) and Mengel et al. (2001) are reliable.

The para-H₂ rates presented in the 30 K panel in Table 1 illustrate the respective contribution of the surface and of the subsequent angular expansion and collisional treatment. Data in columns 1 and 2 are based upon the same JS98 surface and the differences are ascribable to the better convergence of the angular expansion and to the finer description of the resonances. Conversely, data in columns 2 and 3 are based upon the same angular expansion and collisional treatment, and the differences only reflect the improvement in the surface. Depending on initial and final rotation states, various situations may occur. In some cases there is a compensation of errors for the surface (as for 2-1, 3-0, 3-2), or for the expansion and collisional treatment (as for 5-0). Collisional and surface errors may also partially cancel out, as for the 1-0 rate, or add up as for the 2-0 rate. While the detailed behaviour seems complex and irregular, in average the errors introduced by the older JS98 surface are of the same order of magnitude as the errors introduced by the limited angular expansion and energy mesh in the older work by Flower (2001).

It is interesting to note that for collisions with para-H₂, inelastic rates with $\Delta j_1 = 1$ are larger than those with $\Delta j_1 = 2$ while the reverse applies for ortho-H₂. The propensity to favor even Δj_1 over odd Δj_1 has been explained semiclassically by McCurdy & Miller (1977) in terms of an interference effect related to the even anisotropy of the PES. The reverse propensity can also occur if the odd anisotropy is sufficiently large, as observed experimentally in the case of CO-He (Carty et al. 2004). Here, the propensity depends on the quantum state of the projectile because in the para case ($j_2 = 0$), some terms of the PES expansion (those associated with the quadrupole of H₂) vanish identically. Therefore, the even anisotropy of the PES is larger with ortho-H₂ than with para-H₂ and $\Delta j_1 = 2$ are favored. Note, however, that these propensity rules depend on j_1 , Δj_1 and the temperature. Another interesting point is that the differences with the results of Flower (2001) are generally smaller with ortho-H₂ than with para-H₂. This again reflects the different anisotropies of the PES for para and ortho-H₂: in the ortho case, cross sections are larger and scattering calculations are less sensitive to small changes in the PES. Similar effects have also been observed recently in the case of H₂O-H₂ (Dubernet & et al. 2005).

It is also of some interest to compare the present results with the CO-He rates obtained by Cecchi-Pestellini et al.

(2002). It is generally assumed that rates with para-H₂ ($j_2 = 0$) should be about 50% larger than He rates owing to the smaller collisional reduced mass and the larger size of H₂. We have checked that the present H₂ ($j_2 = 0$) rates are in fact within a factor of 1–3 of the He rates. Thus, as already shown by Phillips et al. (1996) in the case of H₂O, rates for excitation by H₂ are not adequately represented by scaled rates for excitation by He.

Finally, for use in astrophysical modelling, the temperature dependence of the above transition rates $k(T)$ have been fitted by the analytic form used by Balakrishnan et al. (1999):

$$\log_{10} k(T) = \sum_{n=0}^4 a_n x^n, \quad (3)$$

where the x factor was changed from $T^{-1/3}$ to $T^{-1/6}$ to achieve a better fitting precision. The quadratic error on this fit is lower than 0.1% for all transitions. The coefficients of this fit are provided as online material. For those who plan to use them, we emphasize that these fits are only valid in the temperature range $5 \leq T \leq 70$ K. Finally, excitation rates are not given in this paper, but can be obtained by application of the detailed balance.

4. Conclusion

Cross sections for the rotational (de)excitation of CO by ground state para- and ortho-H₂ have been computed using quantum scattering calculations for collision energies in the range 1–520 cm⁻¹. A new, highly accurate, CO–H₂ potential energy surface has been employed and it has been shown to strongly influence the resonance structure of the cross sections in the very low collision energy regime ($E_{\text{coll}} \lesssim 60$ cm⁻¹). Conversely, at higher energies, the effect of the new potential was found to be only minor. As a result, the present rate constants are found to differ significantly from those of Flower (2001), obtained on a previous and less accurate potential, only for temperatures lower than 70 K. Transitions among all levels up to $j_1 = 5$ only were computed as higher states are generally not populated at the low temperatures investigated here.

This work illustrates the relationship between the accuracy of the potential energy surface and the accuracy of the corresponding inelastic cross sections for a simple system of astrophysical relevance. Even at low temperatures, moderate inaccuracies in the surface (in the 10-20% range) result in semi-quantitative inelastic rates with typical errors in the 20-50% range with no dramatic amplification of errors. However, this optimistic conclusion presents also a harder counterpart, as we show that in order to obtain accurate inelastic rates one has to satisfy all three conditions, i.e., use an accurate surface, a properly converged angular expansion, and a detailed description of the cross-section resonances. Consequently, the improvement of the accuracy of inelastic rates, especially at higher temperatures when the number of channels is large, represents a considerable computational effort. In this respect, the work by Flower (2001) represented an excellent compromise to achieve a typical 20% accuracy below 100 K.

This work extends the initial objectives of the “Molecular Universe” European FP6 network (2005-2008) and participates

to the current international efforts to improve the description of the underlying microscopic processes in preparation of the next generation of molecular observatories.

Acknowledgements. CCSD(T)-R12 calculations were performed on the IDRIS and CINES French national computing centers (projects no. 051141 and x2005 04 20820). MOLSCAT calculations were performed on an experimental cluster using a subset of the computer grid tools (under project Cigri of the “Action Incitative GRID”) with the valuable help from F. Roch and N. Capit. This research was supported by the CNRS national program “Physique et Chimie du Milieu Interstellaire” and the “Centre National d’Etudes Spatiales”. MW was supported by the Ministère de l’Enseignement Supérieur et de la Recherche. KS acknowledges the NSF CHE-0239611 grant.

References

- Alexander, M. H. & Manolopoulos, D. E. 1987, *J. Chem. Phys.*, 86, 2044
- Antonova, S., Tsakotellis, A. P., Lin, A., & McBane, G. C. 2000, *J. Chem. Phys.*, 112, 554
- Balakrishnan, N., Forrey, R. C., & Dalgarno, A. 1999, *ApJ*, 514, 520
- Balakrishnan, N., Yan, M., & Dalgarno, A. 2002, *ApJ*, 568, 443
- Carty, D., Goddard, A., Sims, I. R., & Smith, I. W. M. 2004, *J. Chem. Phys.*, 121, 4671
- Cecchi-Pestellini, C., Bodo, E., Balakrishnan, N., & Dalgarno, A. 2002, *ApJ*, 571, 1015
- Cernicharo, J., Barlow, M. J., Gonzalez-Alfonso, E., et al. 1996, *A&A*, 315, L201
- Dubernet, M. L. & et al. 2005, in preparation
- Faure, A., Valiron, P., Wernli, M., et al. 2005, *J. Chem. Phys.*, 122, 221102
- Flower, D. R. 2001, *J. Phys. B: At. Opt. Mol. Phys.*, 34, 2731
- Gottfried, J. & McBane, J. C. 2001, *J. Chem. Phys.*, 112, 4417
- Green, S. 1975, *J. Chem. Phys.*, 62, 2271
- Halkier, A., Klopper, W., Helgaker, T., Jørgensen, P., & Taylor, P. R. 1999, *J. Chem. Phys.*, 111, 9157
- Hutson, J. M. & Green, S. 1994, MOLSCAT computer code, version 14 (1994) (distributed by Collaborative Computational Project No. 6 of the Engineering and Physical Sciences Research Council UK)
- Jankowski, P. & Szalewicz, K. 1998, *J. Chem. Phys.*, 108, 3554
- Jankowski, P. & Szalewicz, K. 2005, *The Journal of Chemical Physics*, 123, 104301
- Kedzuch, S., Noga, J., & Valiron, P. 2005, *Mol. Phys.*, 103, 999
- McCurdy, C. W. & Miller, W. H. 1977, *J. Chem. Phys.*, 67, 463
- McGuire, P. & Kouri, D. J. 1974, *J. Chem. Phys.*, 60, 2488
- McKellar, A. R. W. 1998, *J. Chem. Phys.*, 108, 1811
- Mengel, M., de Lucia, F. C., & Herbst, E. 2001, *Canadian Journal of Physics*, 79, 589
- Müller, H. & Kutzelnigg, W. 2000, *Phys. Chem. Chem. Phys.*, 2, 2061
- Noga, J. & Kutzelnigg, W. 1994, *J. Chem. Phys.*, 101, 7738
- Noga, J. & Valiron, P. 2002, in *Computational Chemistry: Reviews of Current Trends*, Vol. 7 (J.Leszczynski ed., World Scientific, Singapore), 131
- Noga, J. & Valiron, P. 2003, *Collect. Czech. Chem. Commun.*, 68, 340
- Phillips, T. R., Maluendes, S., & Green, S. 1996, *ApJS*, 107, 467
- Rist, C., Faure, A., & Valiron, P. 2005, in preparation
- Schinke, R., Engel, V., Buck, U., Meyer, H., & Diercksen, G. H. F. 1985, *ApJ*, 299, 939
- Sims, I. R. 2005, private communication
- Walter, F., Bertoldi, F., Carilli, C., et al. 2003, *Nature*, 424, 406
- Williams, H. L., Mas, E. M., Szalewicz, K., & Jeziorski, B. 1995, *J. Chem. Phys.*, 103, 7374
- Wilson, R. W., Jefferts, K. B., & Penzias, A. A. 1970, *ApJ*, 161, L43+

Table 1. Rotational deexcitation rates of CO in collision with para-H₂ ($j_2 = 0$) at three temperatures. I and F are the CO initial and final rotation states, respectively. All rates are given in units of 10^{-10} cm³/s. Third column recalls the rates of Flower (2001), obtained with the unscaled JS98 surface. Fourth column presents our rates obtained with the JS05 surface. In the 30 K panel, the rates obtained with our expansion of the JS98 surface are also presented.

I	F	Flower	This work
Temp.: 10 K			
1	0	0.281	0.332
2	0	0.229	0.305
3	0	0.064	0.052
4	0	0.020	0.031
5	0	0.007	0.010
2	1	0.697	0.722
3	1	0.412	0.502
4	1	0.114	0.096
5	1	0.042	0.062
3	2	0.816	0.794
4	2	0.526	0.620
5	2	0.153	0.125
4	3	0.888	0.822
5	3	0.656	0.759
5	4	0.925	0.662
I	F	Flower	This work
Temp.: 70 K			
1	0	0.336	0.344
2	0	0.300	0.320
3	0	0.098	0.083
4	0	0.035	0.044
5	0	0.020	0.024
2	1	0.636	0.602
3	1	0.486	0.509
4	1	0.177	0.161
5	1	0.061	0.080
3	2	0.681	0.659
4	2	0.567	0.591
5	2	0.221	0.205
4	3	0.678	0.689
5	3	0.631	0.654
5	4	0.748	0.705

I	F	Flower	This work JS98	This work JS05
Temp.: 30 K				
1	0	0.300	0.288	0.327
2	0	0.269	0.297	0.315
2	1	0.661	0.613	0.612
3	0	0.072	0.059	0.060
3	1	0.456	0.492	0.509
3	2	0.695	0.677	0.670
4	0	0.026	0.029	0.037
4	1	0.130	0.110	0.118
4	2	0.555	0.604	0.612
4	3	0.747	0.716	0.712
5	0	0.010	0.010	0.014
5	1	0.047	0.054	0.068
5	2	0.175	0.149	0.160
5	3	0.648	0.712	0.705
5	4	0.816	0.740	0.713

Table 2. Rotational deexcitation rates of CO in collision with ortho-H₂ ($j_2 = 1$). The conventions are the same as for the para case.

I	F	Flower	This work
Temp.: 10 K			
1	0	0.388	0.379
2	0	0.596	0.559
3	0	0.105	0.071
4	0	0.083	0.061
5	0	0.015	0.016
2	1	0.730	0.712
3	1	0.842	0.831
4	1	0.159	0.124
5	1	0.124	0.105
3	2	0.801	0.748
4	2	0.862	0.894
5	2	0.188	0.150
4	3	0.827	0.786
5	3	0.896	0.972
5	4	0.871	0.695
I	F	Flower	This work
Temp.: 70 K			
1	0	0.402	0.350
2	0	0.629	0.468
3	0	0.114	0.090
4	0	0.079	0.063
5	0	0.027	0.028
2	1	0.684	0.620
3	1	0.858	0.728
4	1	0.199	0.174
5	1	0.124	0.111
3	2	0.732	0.686
4	2	0.871	0.808
5	2	0.236	0.216
4	3	0.757	0.711
5	3	0.880	0.844
5	4	0.779	0.719

Online Material

<i>I</i>	<i>F</i>	<i>a</i> ₀	<i>a</i> ₁	<i>a</i> ₂	<i>a</i> ₃	<i>a</i> ₄
1	0	-10.413	4.162	-20.599	32.563	-16.889
2	0	-9.202	-7.997	18.452	-18.717	6.910
2	1	-0.379	-59.429	131.662	-127.161	45.605
3	0	-3.319	-35.329	53.745	-29.641	2.471
3	1	-7.042	-20.755	48.788	-49.875	18.607
3	2	-1.976	-48.986	107.139	-102.134	36.288
4	0	-8.004	-16.164	28.359	-21.986	6.026
4	1	1.979	-69.801	140.821	-125.047	40.556
4	2	-5.102	-34.014	82.717	-87.211	33.665
4	3	-1.891	-49.861	109.419	-103.434	35.726
5	0	7.564	-106.151	220.187	-205.770	72.462
5	1	-5.209	-32.541	67.718	-63.996	23.105
5	2	4.736	-91.653	203.779	-201.295	73.681
5	3	-5.607	-31.380	78.077	-83.702	32.930
5	4	-0.510	-60.401	137.793	-134.344	46.449

Table .1. Fitting coefficients of CO-para-H₂ rates, following formula 3. *I* and *F* are the initial and final rotation states, respectively. The rates thus obtained are in cm^3/s .

<i>I</i>	<i>F</i>	<i>a</i> ₀	<i>a</i> ₁	<i>a</i> ₂	<i>a</i> ₃	<i>a</i> ₄
1	0	-7.351	-11.062	5.033	16.394	-14.176
2	0	0.331	-68.556	162.123	-167.243	63.863
2	1	4.370	-90.464	207.213	-207.995	77.557
3	0	4.128	-88.472	191.123	-181.945	64.170
3	1	-1.466	-57.252	138.316	-144.752	55.539
3	2	-0.194	-61.716	141.443	-142.699	53.788
4	0	-6.118	-31.232	70.967	-70.685	25.956
4	1	5.330	-96.359	215.047	-212.299	77.662
4	2	-2.940	-49.481	124.615	-135.311	53.609
4	3	-1.454	-53.713	122.102	-121.151	44.472
5	0	5.241	-96.162	206.655	-199.255	72.234
5	1	-6.365	-27.561	61.697	-61.299	22.802
5	2	6.689	-107.753	249.875	-256.409	97.478
5	3	-3.812	-45.669	119.845	-134.502	54.860
5	4	1.082	-71.954	169.486	-173.174	64.402

Table .2. Fitting coefficients of CO-ortho-H₂ rates, following formula 3. *I* and *F* are the initial and final rotation states, respectively. The rates thus obtained are in cm^3/s .